Supporting Information

Contents

1. General information

1.1 Materials

All chemicals were purchased from Shanghai Macklin Biochemical Co., Ltd., Shanghai Bide Medical Technology Co., Ltd. and Guoyao Chemical Reagent Co. Ltd, Shanghai. All chemicals were used without further purification.

1.2 Characterizations

^{1}H NMR and ^{13}C NMR spectra were measured on a **Bruker AVANCE III HD 400 MHz spectrometer (USA)** at room temperature with tetramethylsilane (TMS) as reference. Methanol-d_4 (CD_3OD) and chloroform-d ($CDCl_3$) were used as solvent. High-resolution mass spectrometry (HRMS) was performed via **Agilent Q-TOF 6510 MS spectrometer (USA)**. Transmission electron microscope (TEM) images were measured by a **HITACHI JEM-100CX II electron microscope (Japan)**. The samples for TEM detection were dropped in the copper grid and air-dried. Scanning electron microscope (SEM) images were measured by a **Zeiss scanning electron microscope**

(Germany). The samples for SEM detection were dropped in the silicon pellet, dried and then sprayed by the gold before detection. Circular dichroism (CD) and circularly polarized luminescence (CPL) were measured with **Applied Photophysics Chirascan V100 (UK)**:

light source: 150W Xenon lamp, 150W Mercury Xenon lamp, effective measurement wavelength range: ≥ 170～1200 nm, wavelength accuracy: ± 0.1nm (163～500nm), ± 0.5nm (500～1200nm), wavelength resolution: ≤ 0.025nm, baseline stability: no more than 0.03 mdeg/hr, CD resolution: ≤ 0.00001, CD measurement range: ≥ ± 8000 mdeg. Grazing incidence wide-angle X-ray scattering (GIWAXS) measurements were conducted at a **Xeuss 3.0 SAXS/WAXS** laboratory beamline at Vacuum Interconnected Nanotech Workstation (Nano-X) from Suzhou Institute of Nano-Tech and Nano-Bionics, Chinese Academy of Sciences in China with Kα X-ray of Cu source (operated at 50kV, 0.06 mA, 1.542 Å). GIWAXS patterns were recorded by a two dimensional X-ray detector (Eiger2 R 1M, Dectris). The incident angle was set to 0.2 degree. Powder X-ray diffraction (XRD) patterns were collected on a **PANalytical (X'Pert3 Powder&XRK-900)**. X-ray diffraction (UK) with Cu Kα radiation (λ = 0.15406 nm, voltage 45 kV, current 200 mA, power 9 KW). Fluorescent spectra were recorded via a **RF-6000 from SHIMADZU**.

1.3 Assembly methods

The compounds **1-12** were each dissolved in THF to prepare concentrated stock solutions (10 mM). To induce co-assembly, the required volumes of stock solutions were mixed according to the designed ratios, followed by the addition of deionized water. Using the **1•2** co-assemble as an example: compounds **1** and **2** were first dissolved in THF to obtain 10 mM stock solutions. Then, 100 μL of the stock solution of **1** and 100 μL of the stock solution of **2** were transferred into a 1 mL vial using micropipettes and gently shaken to ensure thorough mixing. After forming a homogeneous mixture, the solvent was evaporated completely in the dark.

Subsequently, THF (100 μL) and deionized water (900 μL) were added to the dried residue, and the vial was sealed with a cap and parafilm. The mixture was gently shaken

to obtain a homogeneous solution (final concentration ratio: 1:2 = 1 mM : 1 mM). The system was then allowed to age at room temperature for at least 12 hours to ensure completion of the self-assembly process. The aged solution was used for CD and CPL measurements.

Other co-assembled systems were prepared following the same procedure, with appropriate adjustments made according to the required molar ratios.

The films of GIXS were prepared using a nanoprecipitation method followed by a 12-hour assembly process. After assembly, the aggregates were collected by high-speed centrifugation, and the resulting precipitates were cast onto silicon wafers and allowed to dry naturally. During drying, the chiral nanofibers-with their characteristic aspect ratios-tended to sediment and align parallel to the wafer surface, facilitating uniform film formation.

1.4 Molecular dynamic (MD) simulation

The geometries of **1** and acid were constructed and initially optimized by the Gaussian View06 program, and the electrostatic potential (ESP) was simultaneously calculated by Hartree–Fork method at the B3LYP/6-31G (d,p) basis. The Antechamber program was used to fit the restrained electrostatic potential (RESP) charge, and then the general Amber force field (GAFF) was adopted to parameterize the for subsequent MD simulations. The topology files of molecules were parametrized under the corroboration of the GROMACS force field using Amber, ACPYPE, and Guassian tools.

The MD simulation of the self-assembly system was carried out as follows. We built a box with a length, width, and height of 20×20×20 nm^3, respectively. And we inserted 600 **1** molecules into the box by free dispersing.

The MD simulation of the co-assembly system was carried out as follows. We built a box with a length, width, and height of 10×10×10 nm^3, respectively. And we inserted 200 **1** molecules into the box by free dispersing. Then, 100 **3** (or **7**) molecules were inserted into the box.

Followed by filling with solvents (the water solvent simulated was the SPC216 model), the MD simulation of the co-assembly system was carried out for 15 ns under 298 K.

The simulations were achieved by the GROMACS 2020 program. All the number of H-bonds, solvent accessible area and Radical function (RDF) were calculated by the results based on MD calculation.

1.5 Synthesis

Synthesis of Compound 1

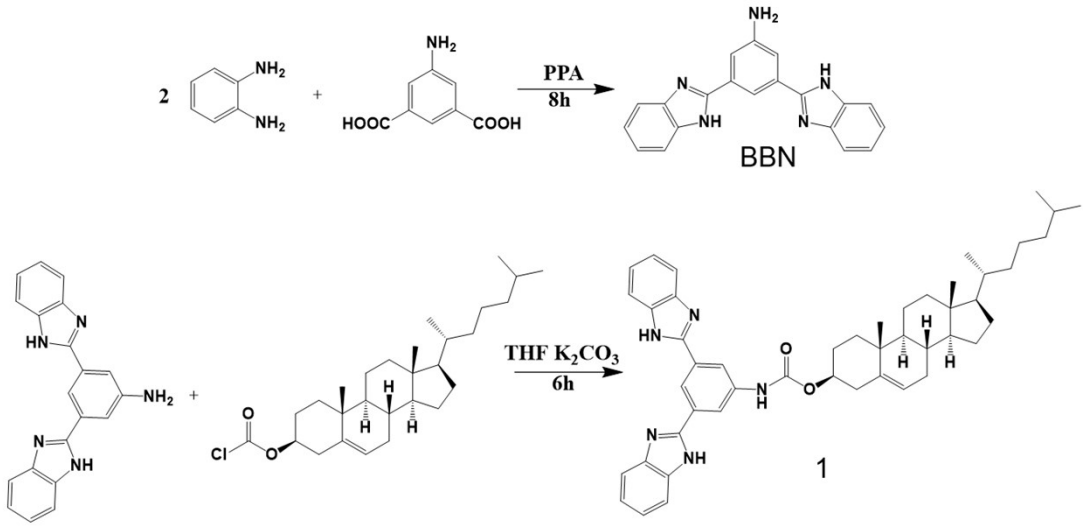

Figure S1. The synthetic route of **1**.

Synthesis of compound BBN: 5-Aminoisophthalic acid (2mol 0.362g) and o-phenylenediamine (4.2 mol 0.454 g) were added to 250 ml round-bottled flask. Then PPA was added to completely cover the powder. And the whole mixture was stirred for 8 h at 180 ℃. After completion of reaction, the mixtures were poured into a 1000 ml beaker filled with ice water and stir thoroughly. After stirring, filter, the residue was added into a 1000 ml beaker filled with saturated $NaHCO_3$, which were stirred and filtered. Then the filtered residues were washed by DI water to get the crude product of BBN.

Synthesis of compound 1: BBN (1 mmol 0.325g) and excess K_2CO_3 was added to 250 ml brown round-bottomed flask and appropriate amount of THF was added. Cholesterol chloroformate (1.2 mmol 0.539g) was added to 100 ml beaker, where THF was added to dissolve it completely, which was dropwise added to the above mixture at room

temperature. After the reaction was completed for 6h. Compound **1** was further purified by silica gel column chromatography. ^{1}H NMR (400 MHz, Chloroform-d) δ 8.27 (s, 1H), δ 8.16 (s, 2H), 7.65 – 7.58 (m, 4H), 7.26 (dd, J = 6.2, 3.1 Hz, 4H), 2.44 – 2.35 (m, 2H). 13C NMR (101 MHz, Chloroform-d) δ 153.29, 150.07, 139.34, 138.73, 130.04, 122.13, 121.75, 117.55, 116.63, 74.28, 70.55, 55.75, 55.17, 49.14, 49.10, 48.93, 48.72, 48.51, 48.30, 48.08, 47.87, 47.65, 41.33, 41.07, 38.76, 38.53, 37.48, 36.01, 35.64, 35.51, 35.20, 34.80, 30.95, 30.87, 30.40, 29.17, 28.70, 28.36, 27.24, 27.08, 27.02, 23.29, 22.85, 21.80, 21.69, 21.54, 20.07, 18.32, 18.17, 17.71, 13.09, 10.86. HRMS (TOF) m/z $[M+H]^{+}$, calcd for $C_{48}H_{59}N_5O_2$, 738.4669; found, 738.4729.

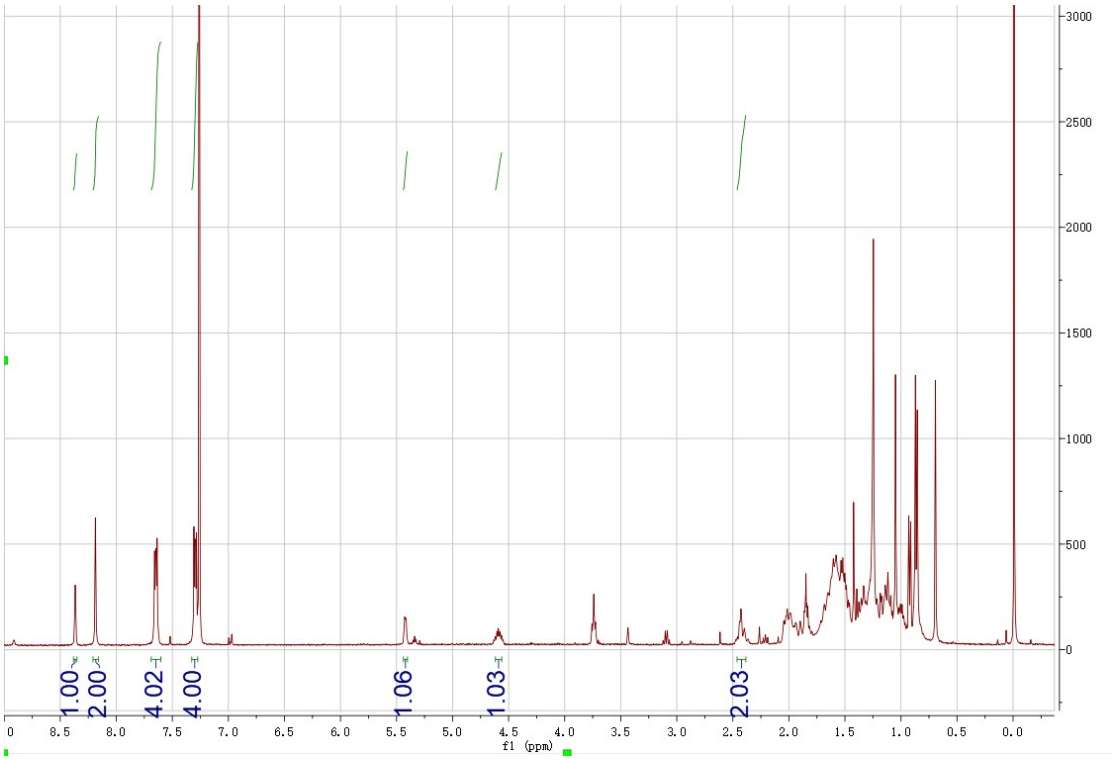

Figure S2. ^{1}H NMR spectrum of **1** in $CDCl_3$

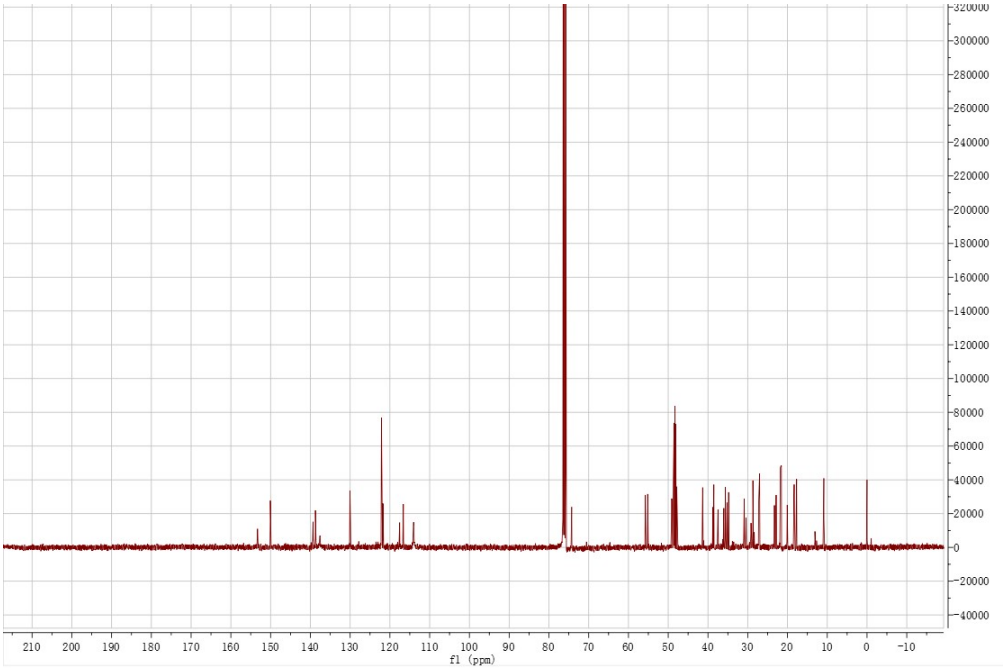

Figure S3. ^{13}C NMR spectrum of **1** in $CDCl_3$

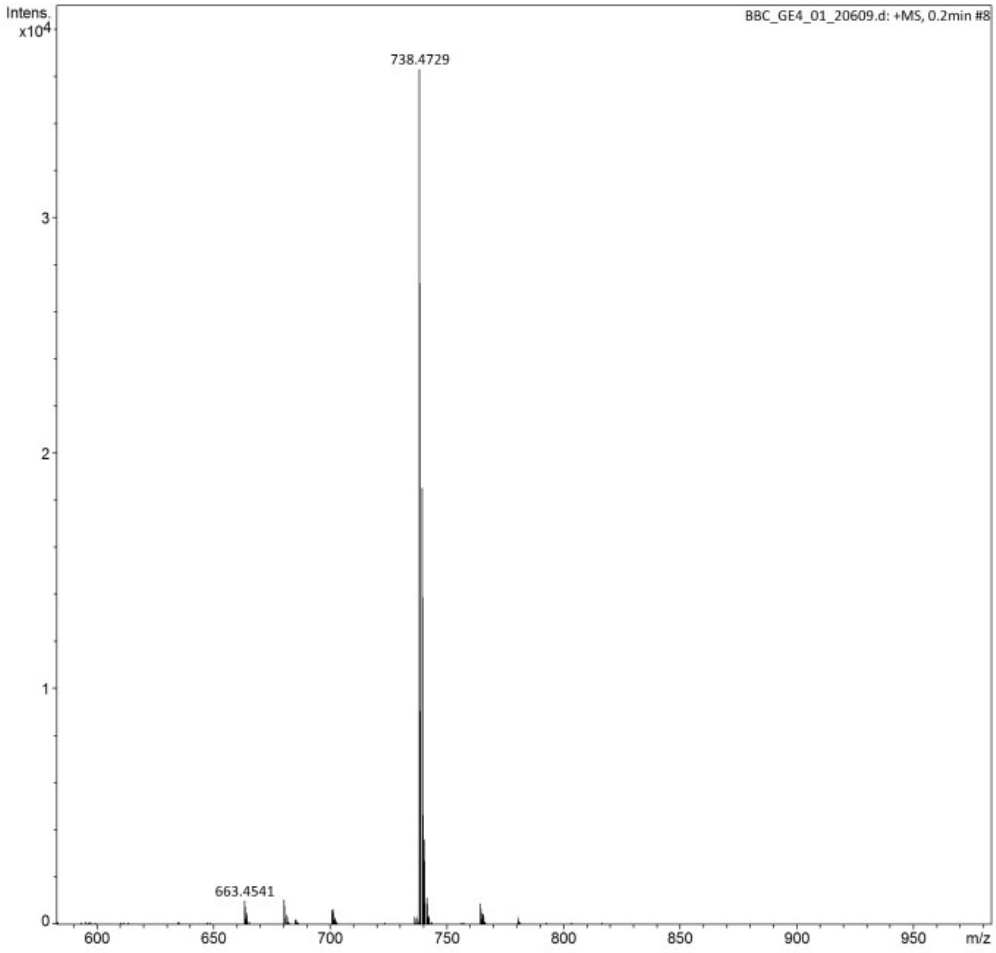

Figure S4. HR-MS spectrum of **1**.

2. Additional experimental results

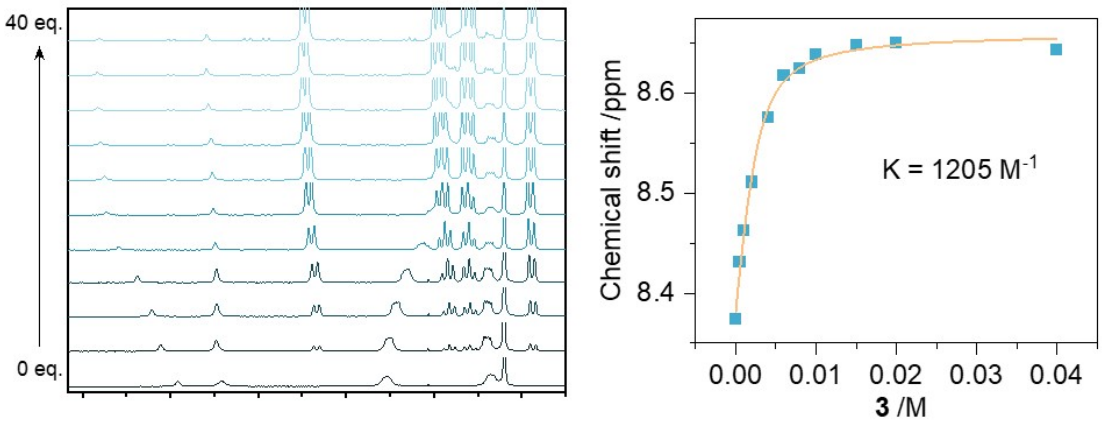

Figure S5. ^{1}H NMR titration of **1•3** in $CDCl_3$ with 5 vol% CD_3OD. And fitted ^{1}H NMR curves with calculated apparent binding constant K for **1•3.**

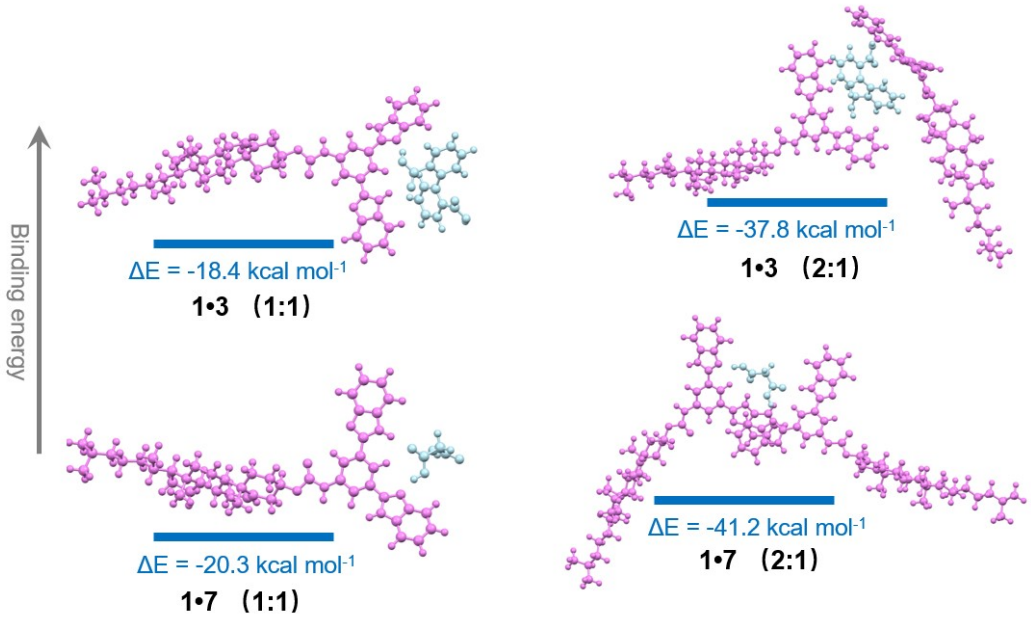

Figure S6. Binding energies of **1•3** and **1•7** with 1:1 and 1:2 binding stoichiometry.

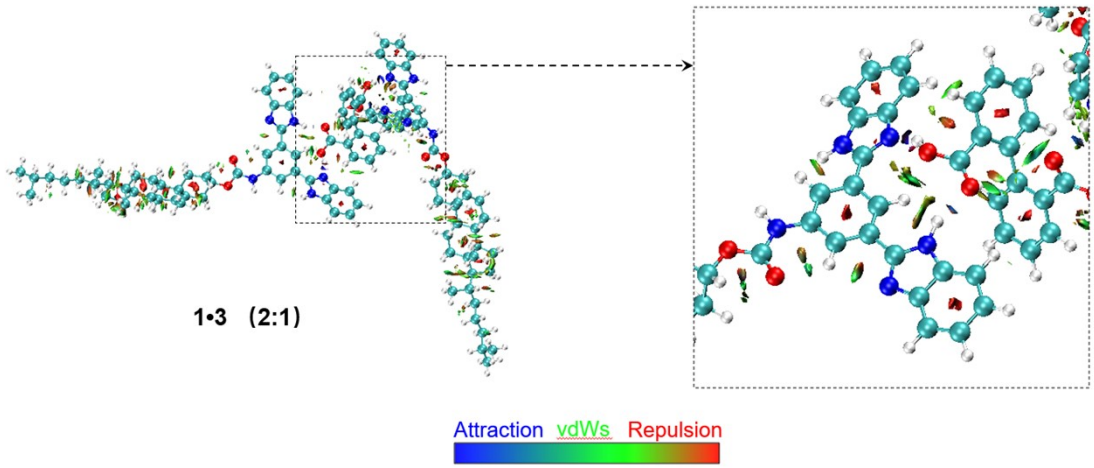

Figure S7. NCI analysis of **1•3** with 2:1 binding stoichiometry. Basis set: b3lyp/6-311g(d).

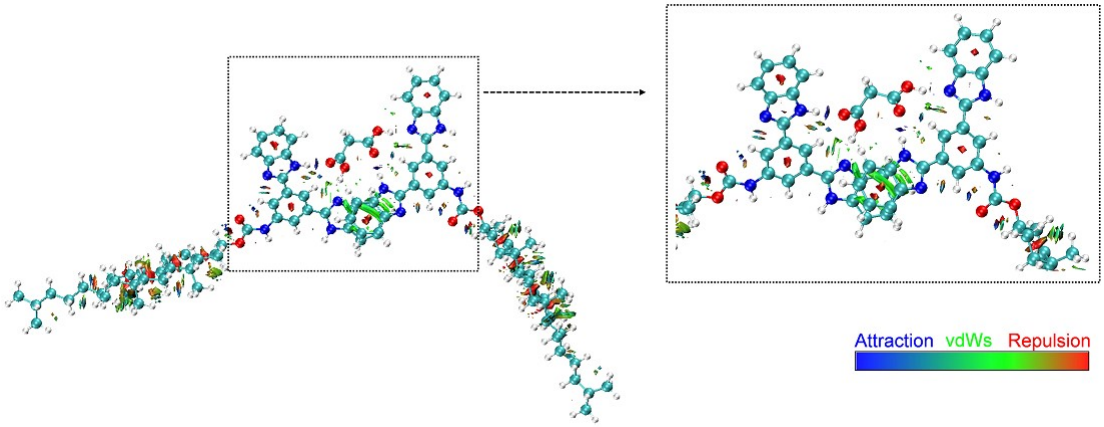

Figure S8. NCI analysis of **1•7** with 2:1 binding stoichiometry. Basis set: b3lyp/6-311g(d).

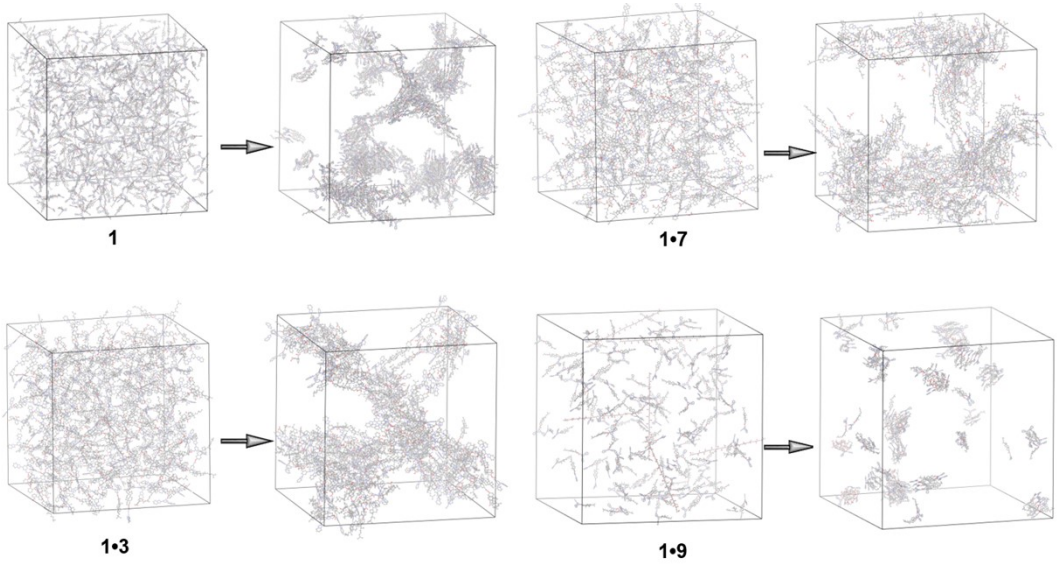

Figure S9. MD results. Aggregation behaviors within the simulation boxes of 0 ns and 150 ns for comparison.

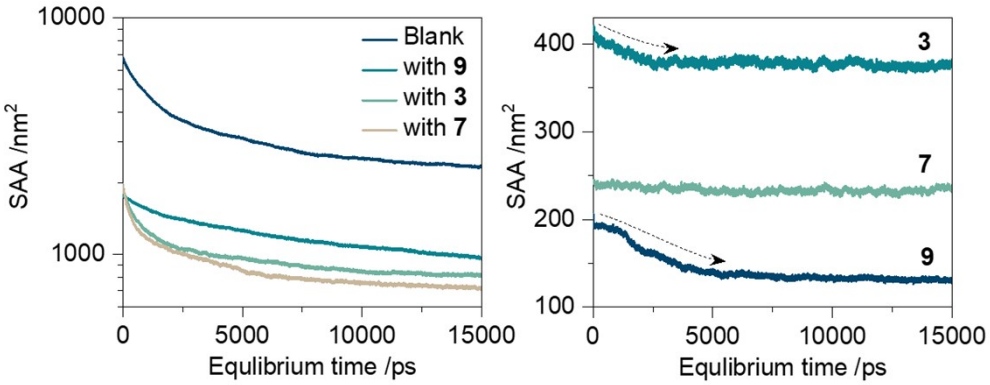

Figure S10. SAA changes with equilibrium time in **1•3**, **1•7** and **1•9** systems.

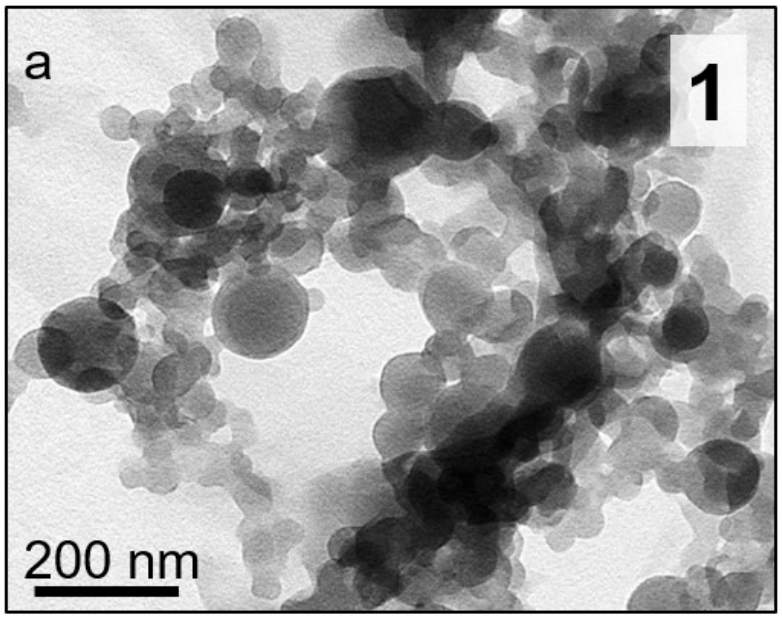

Figure S11. TEM images of self-assembled compound **1** (1 mM)

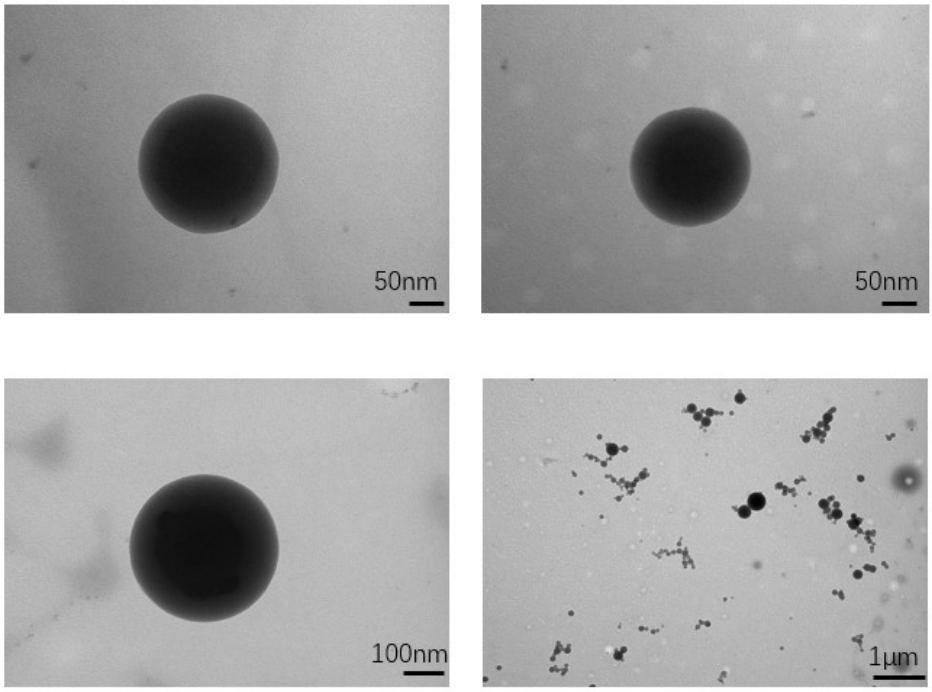

Figure S12. TEM images of self-assembled compound **1** (1 mM).

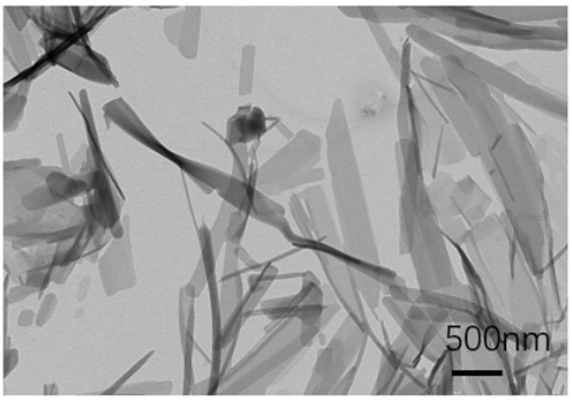

Figure S13. TEM images of coassembled compound **1** (1 mM) with **2**. Molar ratio is 1:2. Water fraction f_w is 90 vol%.

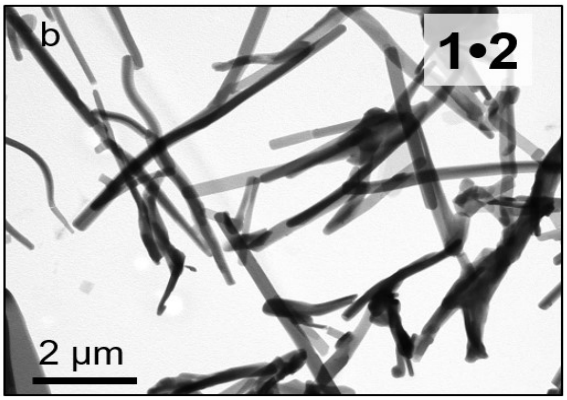

Figure S14. TEM images of coassembled compound **1** (1 mM) with **2**. Molar ratio is 1:2. Water fraction f_w is 80 vol%.

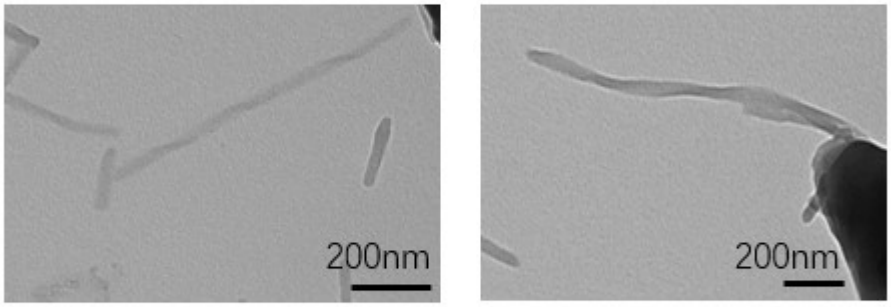

Figure S15. TEM images of coassembled compound **1** (1 mM) with **3**. Molar ratio is 1:1. Water fraction f_w is 90 vol%.

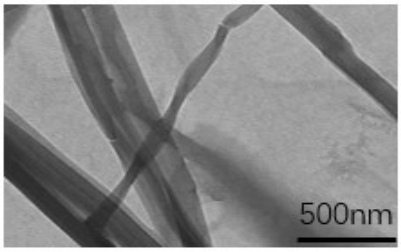

Figure S16. TEM images of coassembled compound **1** (1 mM) with **3**. Molar ratio is 1:1. Water fraction f_w is 80 vol%.

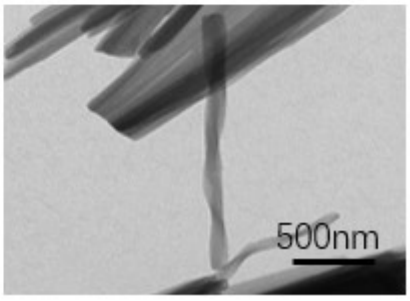

Figure S17. TEM images of coassembled compound **1** (1 mM) with **3**. Water fraction f_w is 70 vol%.

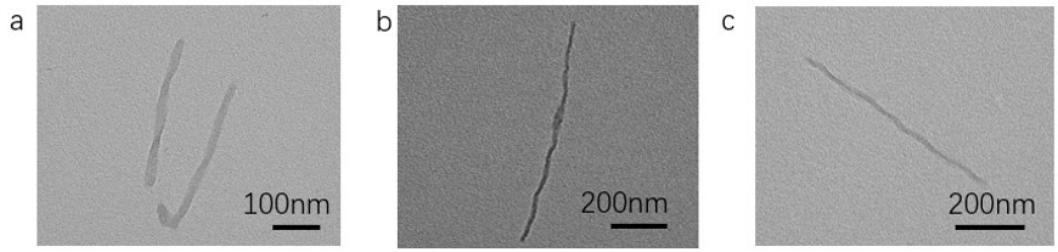

Figure S18. TEM images of coassembly compound **1** (1 mM) with **4**. (a, b, c) Molar ratio is 1:0.66. Water fraction f_w is 90 vol%

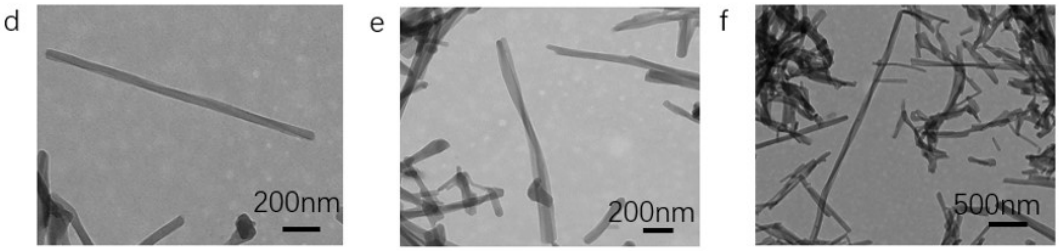

Figure S19. TEM images of coassembly compound **1** (1 mM) with **4**. (d, e, f) Molar ratio is 1:0.66. Water fraction f_w is 80 vol%.

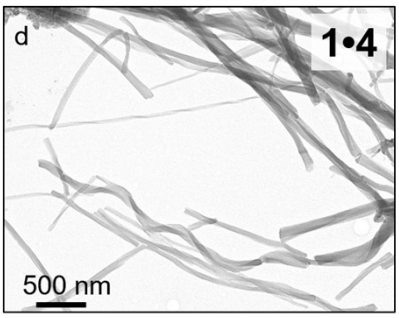

Figure S20. TEM images of coassembled compound **1** (1 mM) with **4**. Molar ratio is 1:0.66. Water fraction f_w is 70 vol%

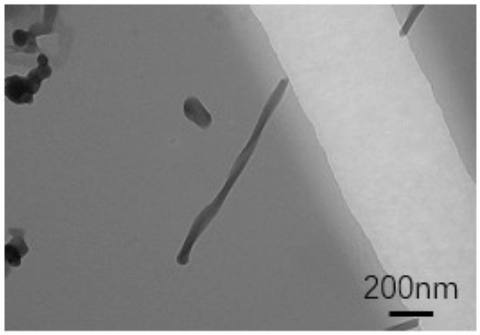

Figure S21. TEM images of coassembled compound **1** (1 mM) with **5**. Molar ratio is 1:0.5. Water fraction f_w is 90 vol%.

Figure S22. TEM images of coassembled compound **1** (1 mM) with **5**. Molar ratio is 1:0.5. Water fraction f_w is 80 vol%.

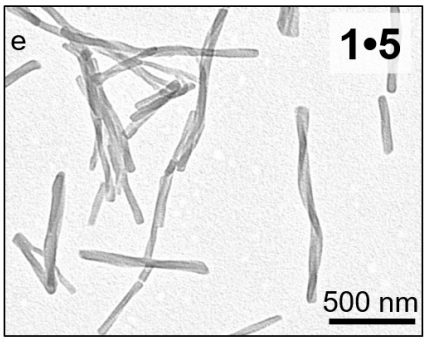

Figure S23. TEM images of coassembled compound **1** (1 mM) with **5**. Molar ratio is 1:0.5. Water fraction f_w is 70 vol%.

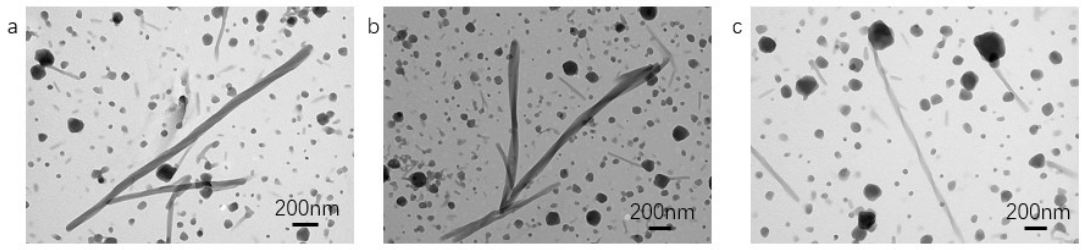

Figure S24. TEM images of coassembled compound **1** (1 mM) with **6**. Molar ratio is 1:1. Water fraction f_w is 90 vol%.

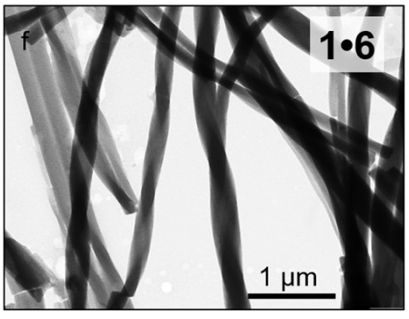

Figure S25. TEM images of coassembled compound **1** (1 mM) with **6**. Molar ratio is 1:1. Water fraction f_w is 80 vol%.

Figure S26. TEM images of coassembled compound **1** (1 mM) with **6**. Molar ratio is 1:1. Water fraction f_w is 70 vol%.

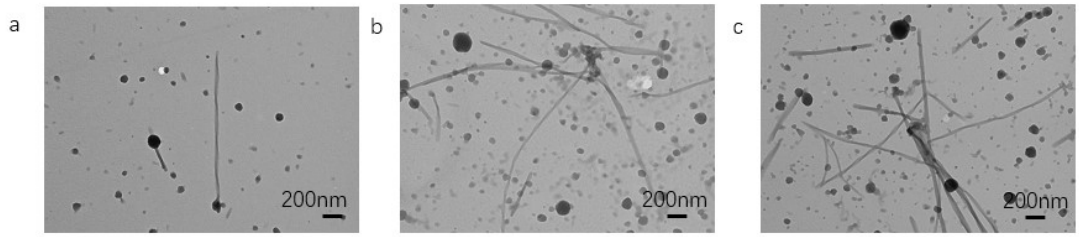

Figure S27. TEM images of coassembly compound **1** (1 mM) with **7**. Molar ratio is 1:1. Water fraction f_w is 90 vol%.

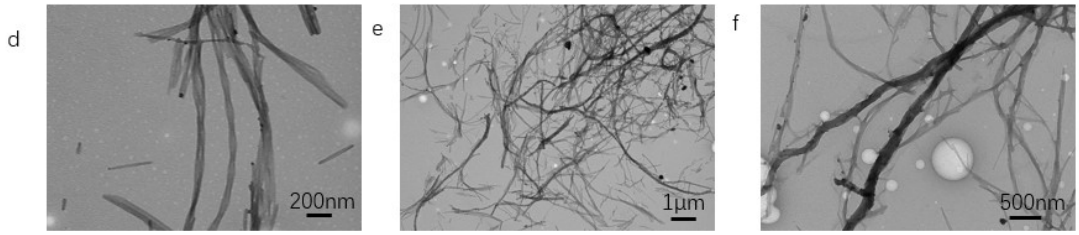

Figure S28. TEM images of coassembly compound **1** (1 mM) with **7**. Molar ratio is 1:1. Water fraction f_w is 80 vol%.

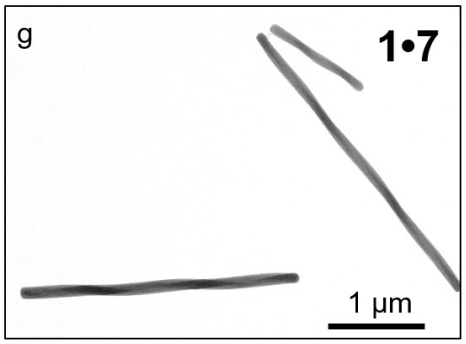

Figure S29. TEM images of coassembled compound **1** (1 mM) with **7**. Molar ratio is 1:1. Water fraction f_w is 70 vol%.

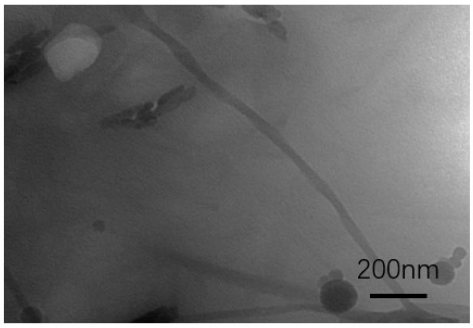

Figure S30. TEM images of coassembled compound **1** (1 mM) with **8**. (a) Molar ratio is 1:1. Water fraction f_w is 90 vol%.

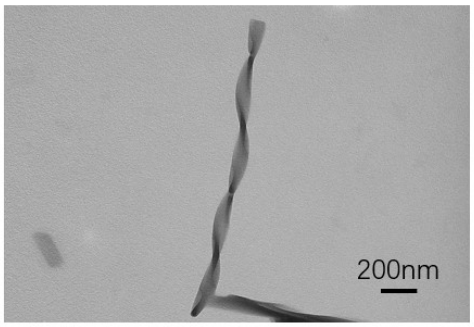

Figure S31. TEM images of coassembled compound **1** (1 mM) with **8**. Molar ratio is 1:1. Water fraction f_w is 80 vol%.

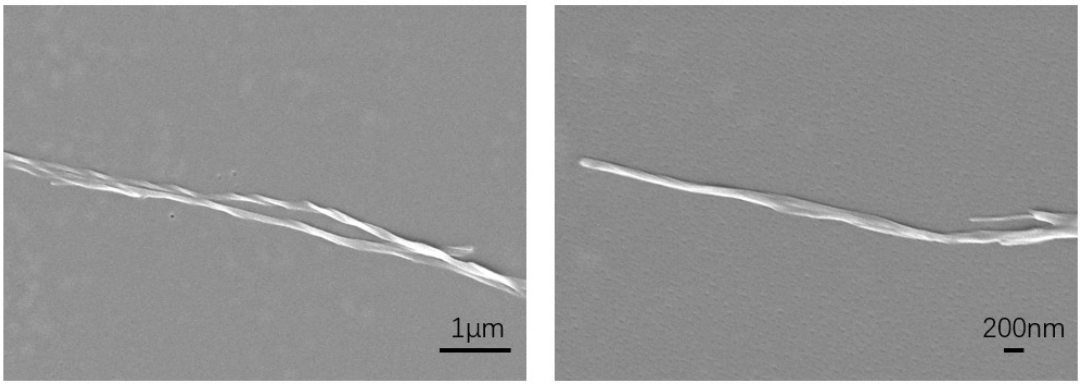

Figure S32. SEM images of **1•4** (f_w = 70 vol%, 1:0.66)

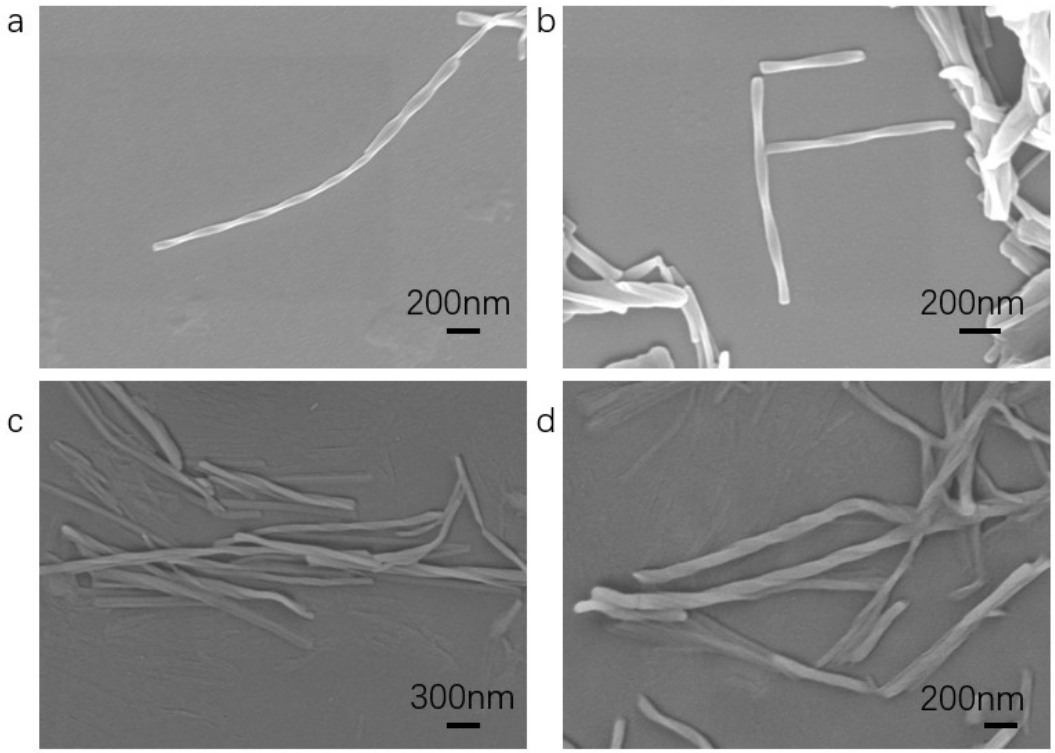

Figure S33. SEM images of **1•5** (a, b) f_w = 80 vol%, 1:0.5 (c, d) f_w = 80 vol%, 1:1.25.

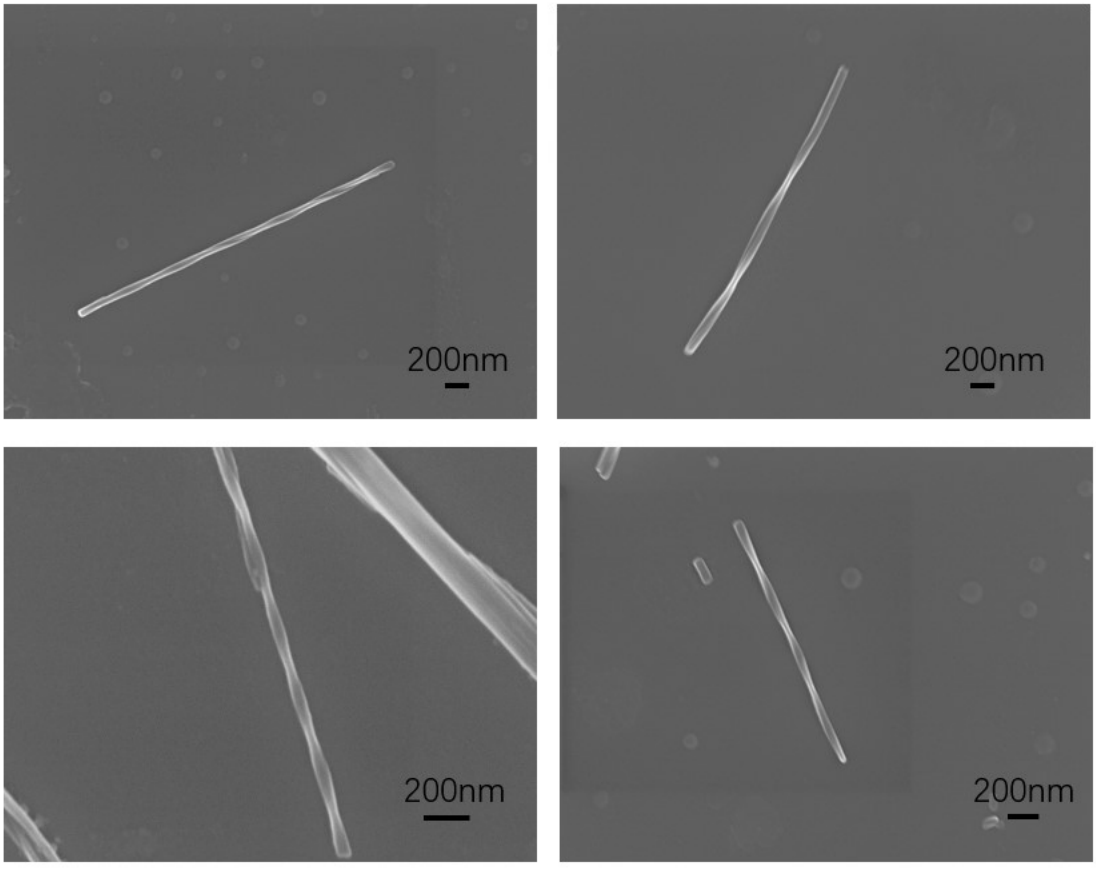

Figure S34. SEM images of **1•6** f_w = 80 vol%, 1:1

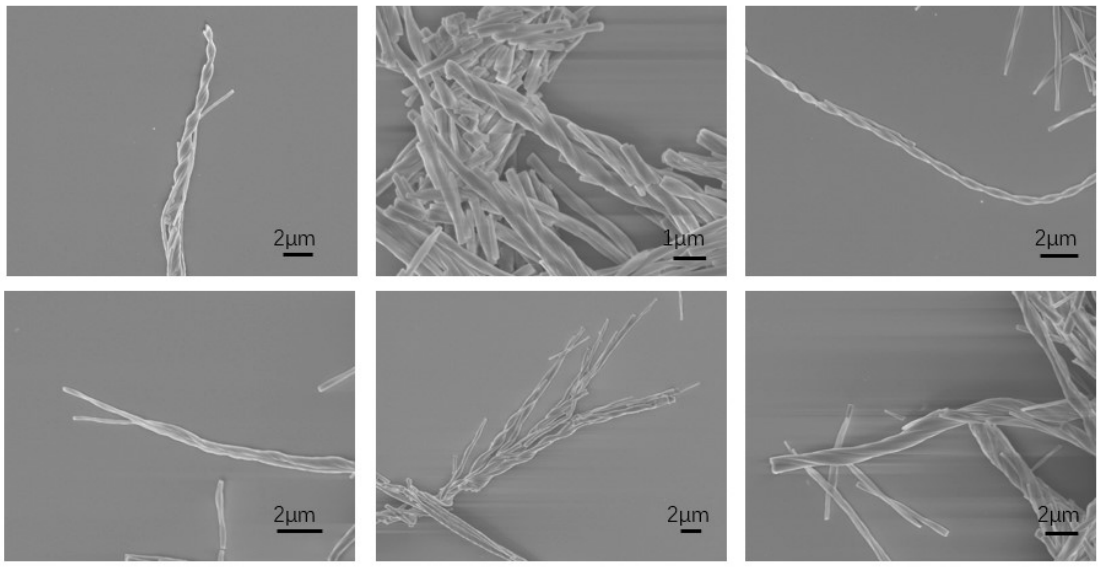

Figure S35. SEM images of **1•7**, f_w = 80 vol%, 1:1

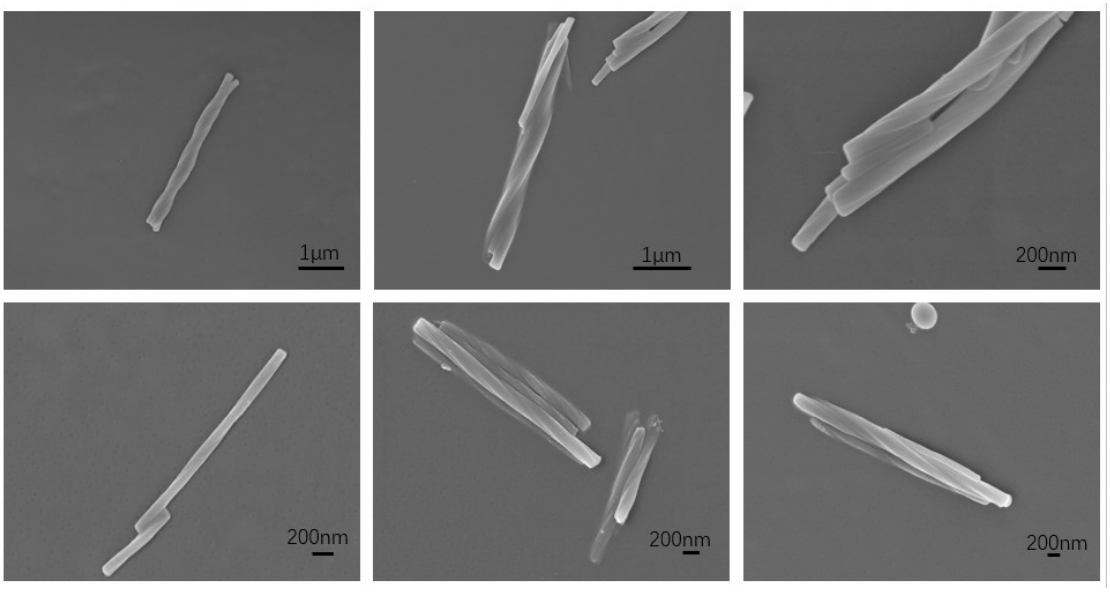

Figure S36. SEM images of **1•7**, f_w = 70 vol%, 1:1.

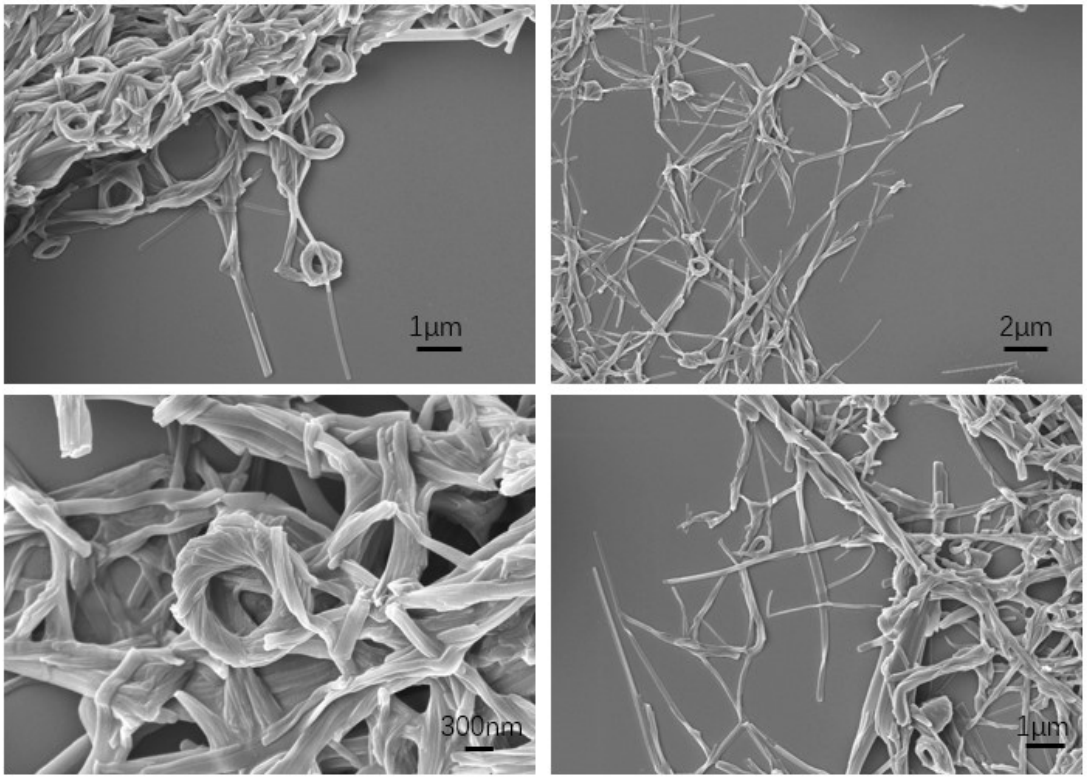

Figure S37. SEM images of **1•7**, f_w = 80 vol%, 1:2.5.

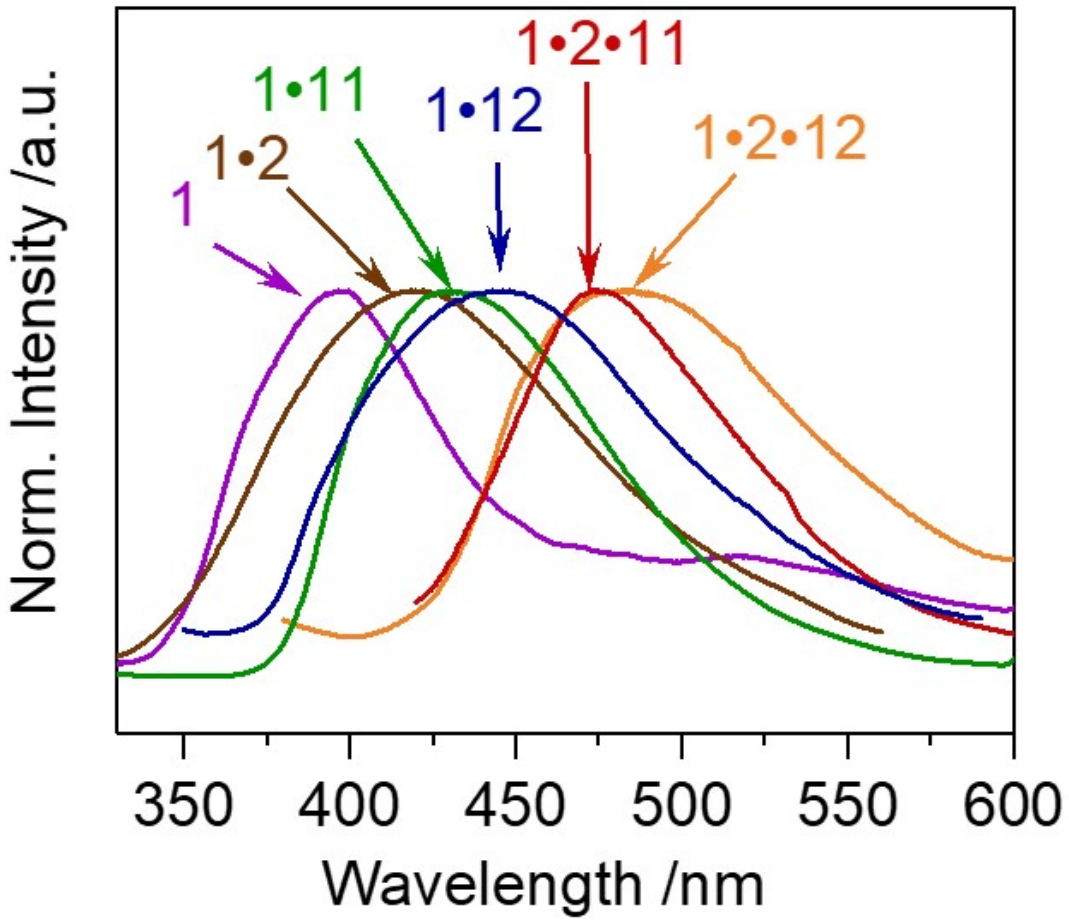

Figure S38. Fluorescence spectra of different components. **1**, **1•11**, **1•12** (λ_{ex} = 310 nm), **1•2**, **1•2•11**, **1•2•12** (λ_{ex} = 340 nm).

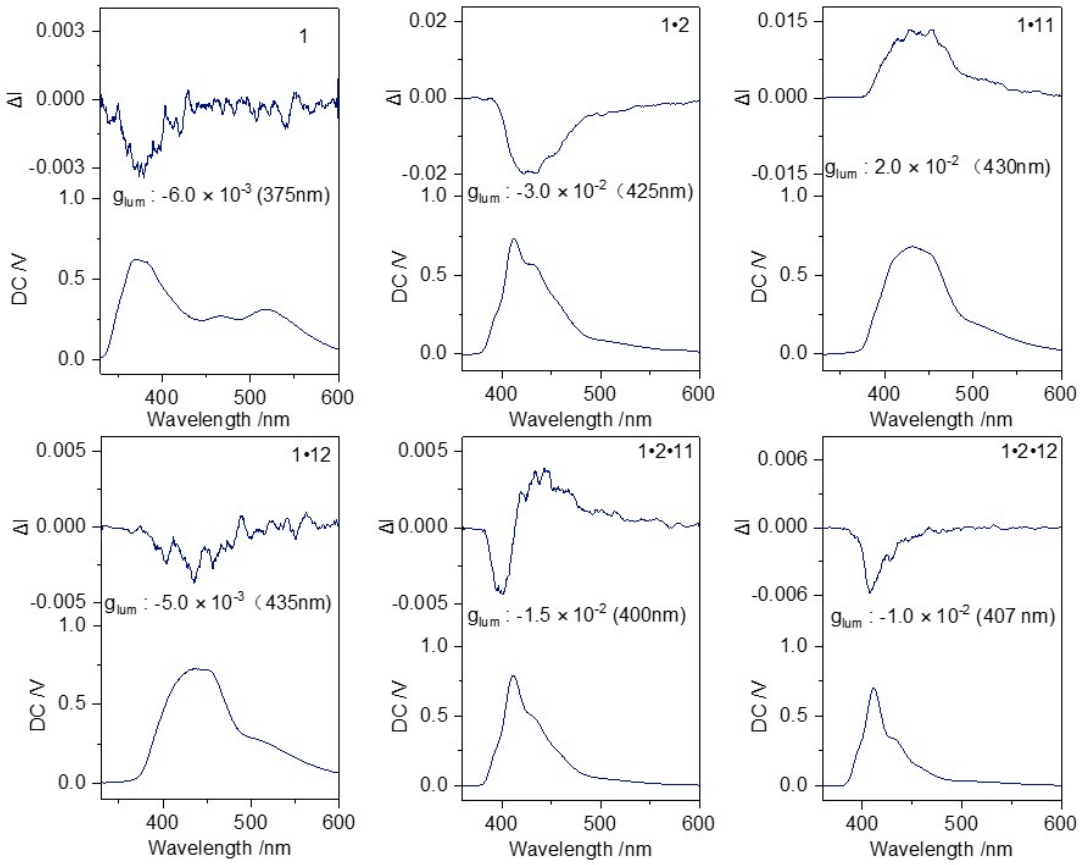

Figure S39. CPL of different components.

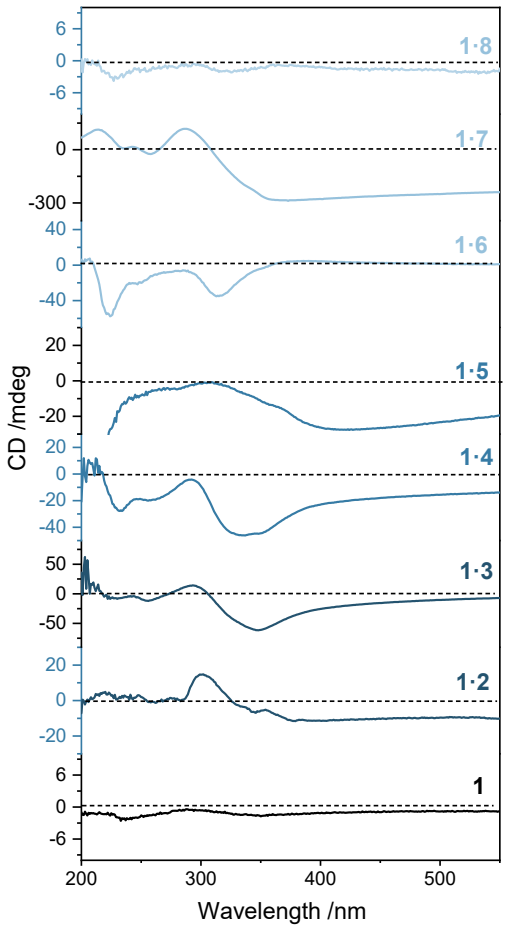

Figure S40. Representative CD spectra of self-assembled compound **1** (1 mM) as well as the coassembly with **2**-**8** respectively. Molar ratios are 1:0, 1:2, 1:2.5, 1:0.66, 1:0.5, 1:1, 1:1 and 1:1 respectively. Water fraction f_w are 80 vol%, 80 vol%, 80 vol%, 70 vol%, 90 vol%, 90 vol%, 80 vol% and 80 vol%.

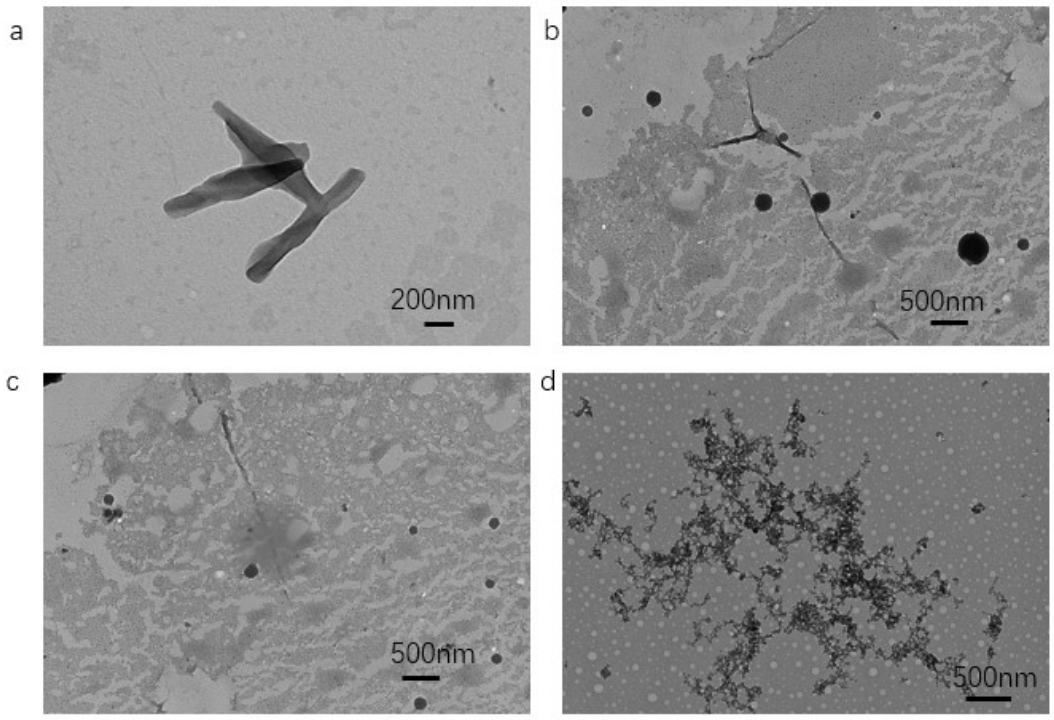

Figure S41. (a)TEM images of **1•9** coassemblies (c = 1 mM, ratio = 1: 5, based on the monomer, f_w = 90 vol%). (b, c) TEM images of **1•9** coassemblies (c = 1 mM, ratio = 1: 5, based on the monomer, f_w = 80 vol%). (d) TEM images of **1•9** coassemblies (c = 1 mM, raito = 1: 5, based on the monomer, f_w = 70 vol%)

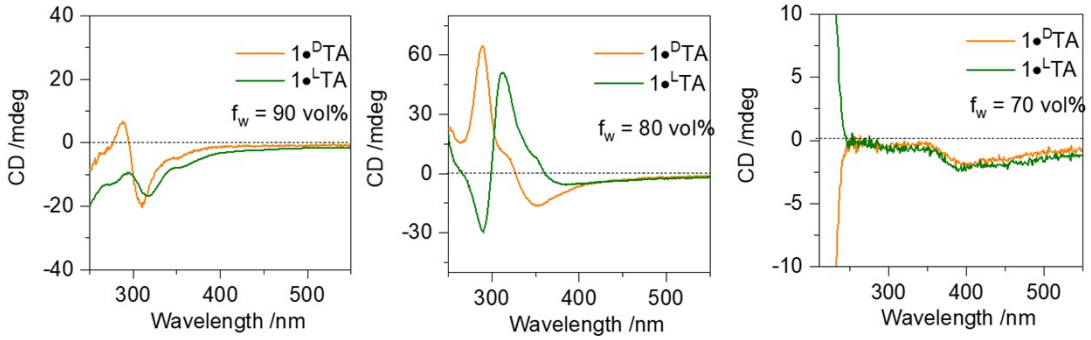

Figure S42. Water fraction-dependent CD spectra of enantiomeric pure **1•TA** (1:1 by molar) coassemblies.

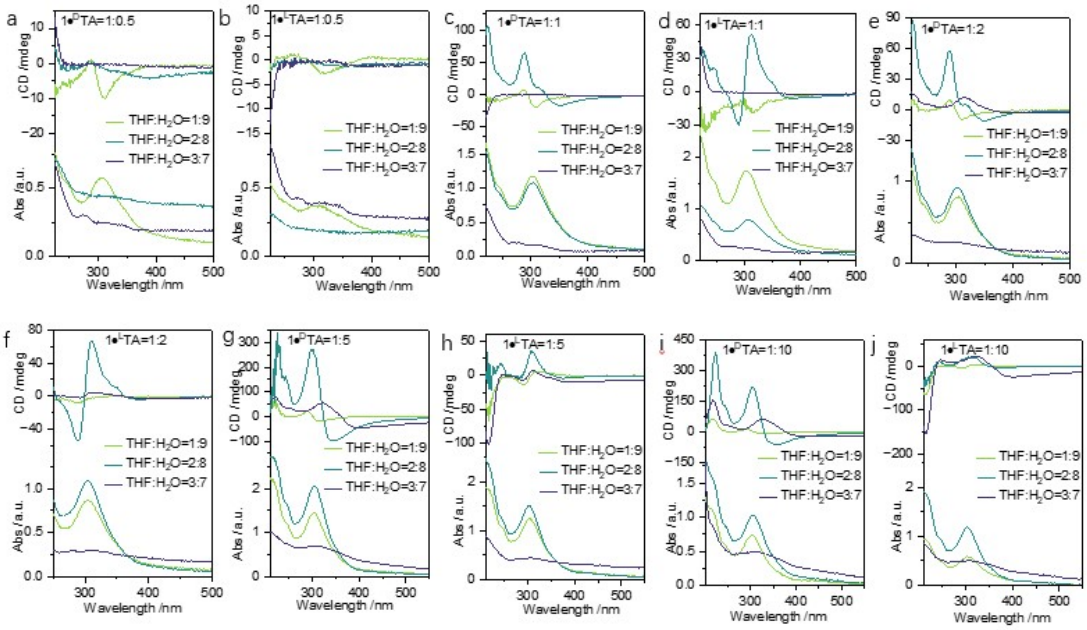

Figure S43. Water fraction-dependent CD spectra of enantiomeric pure **1•TA** coassemblies. (a, b) **1•TA** ratio = 1: 0.5. (c, d) **1•TA** ratio = 1: 1. (e, f) **1•TA** ratio = 1: 2. (g, h) **1•TA** ratio = 1: 5. (i, j) **1•TA** ratio = 1: 10.

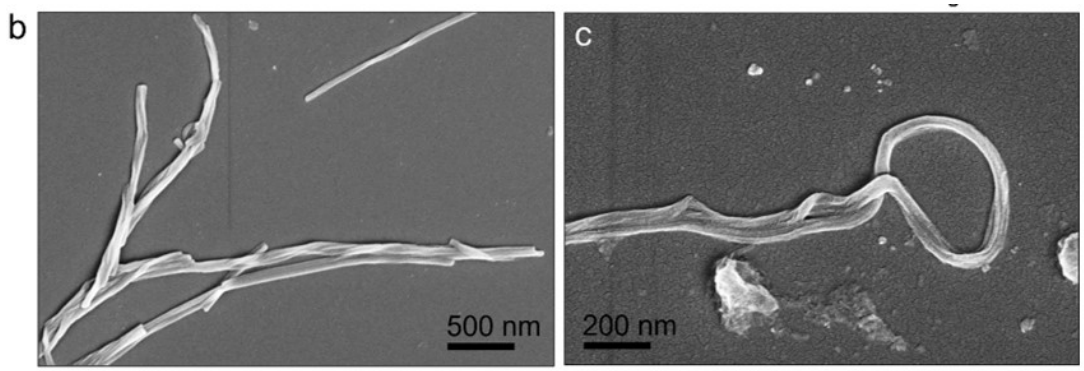

Figure S44. b,c) SEM image of **1•^{L}TA** and **1•^{D}TA** (f_w = 70 vol%, 1:10 by molar) coassemblies.

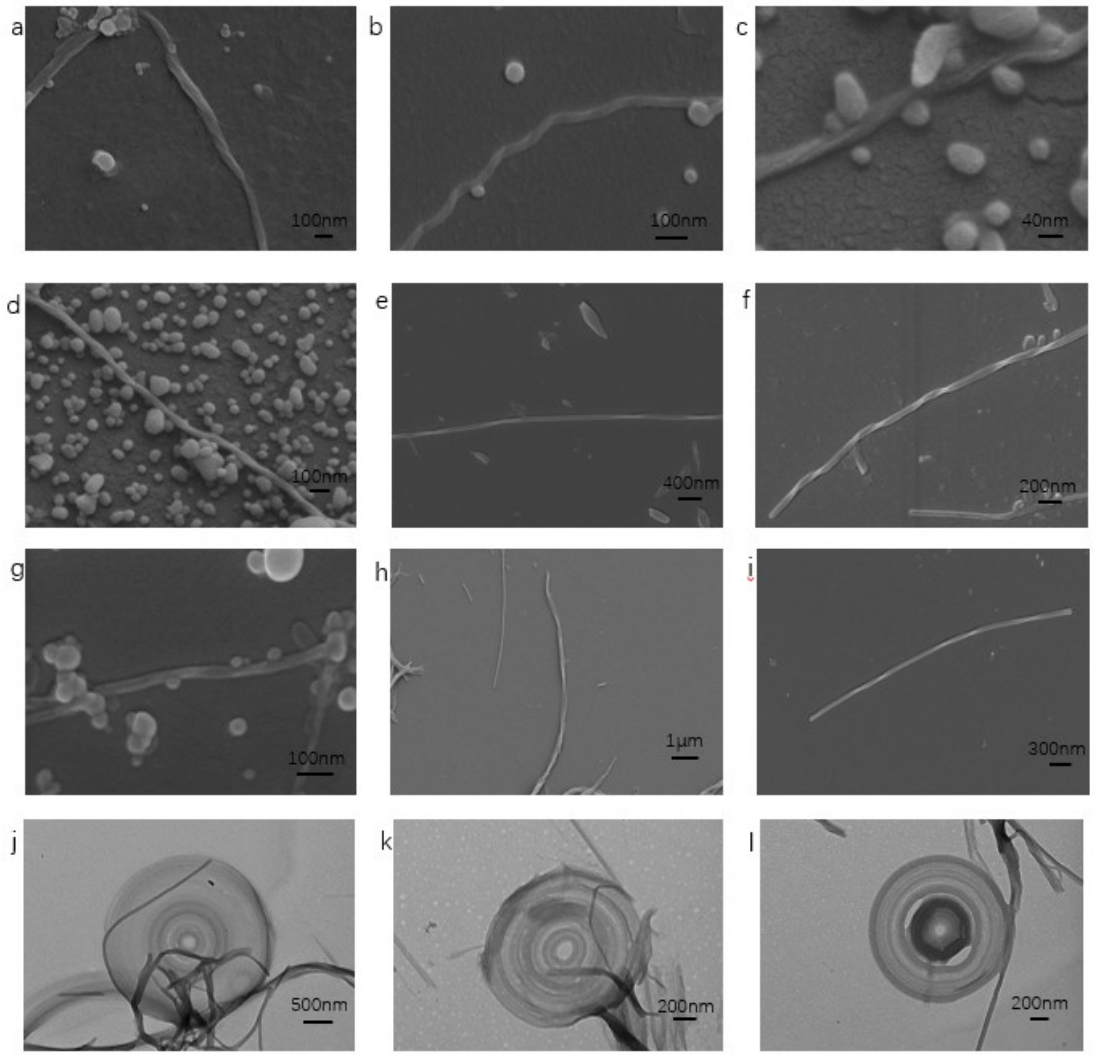

Figure S45. (a) SEM image of **1•^{D}TA** (f_w = 90 vol%, 1:1 by molar) coassemblies. (b) SEM image of **1•^{D}TA** (f_w = 90 vol%, 1:2 by molar). (c) SEM image of **1•^{D}TA** (f_w = 80 vol%, 1:2 by molar). (d) SEM image of **1•^{L}TA** (f_w = 80 vol%, 1:2 by molar). (e) SEM image of **1•^{D}TA** (f_w = 70 vol%, 1:2 by molar). (f) SEM image of **1•^{L}TA** (f_w = 70 vol%, 1:3 by molar). (g) SEM image of **1•^{D}TA** (f_w = 90 vol%, 1:5 by molar). (h) SEM image of **1•^{D}TA** (f_w = 70 vol%, 1:5 by molar). (i) SEM image of **1•^{D}TA** (f_w = 70 vol%, 1:10 by molar). (j-l) TEM image of **1•^{L}TA** (f_w = 70 vol%, 1:10 by molar)

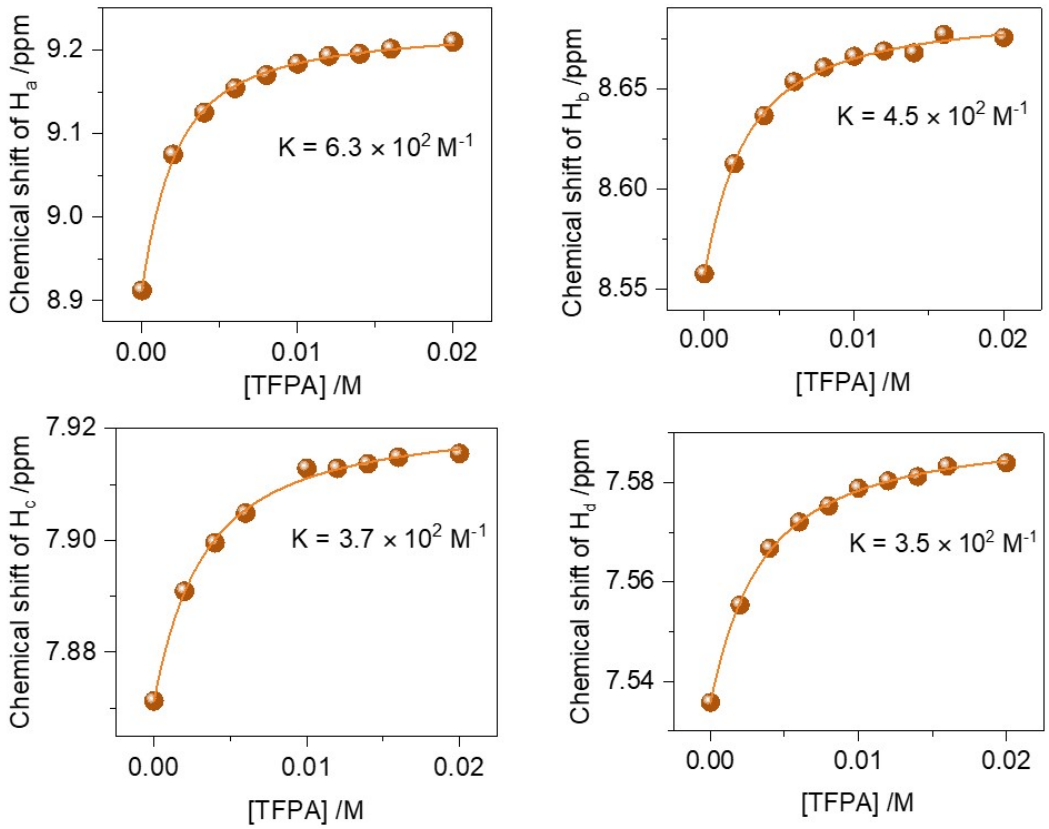

Figure S46. ^{1}H NMR comparison of **1•11** system measured in $CDCl_3$ with **5** vol% CD_3OD.

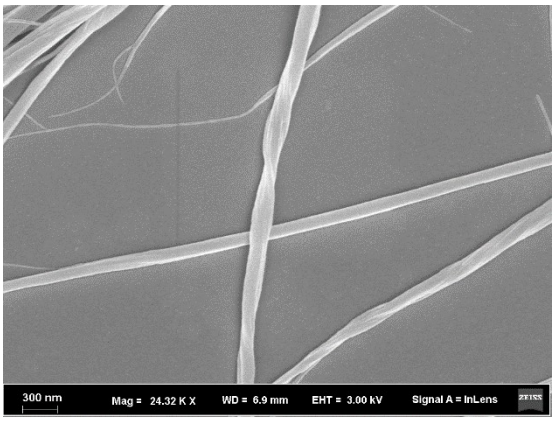

Figure S47. SEM images of **1•2** (f_w = 80 vol%, 1:1).

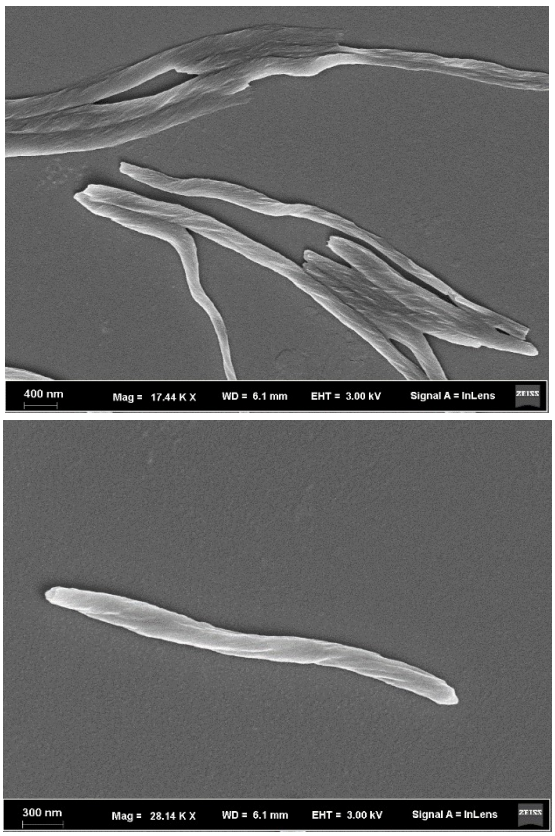

Figure S48. SEM images of **1•11** (f_w = 80 vol%, 1:1).

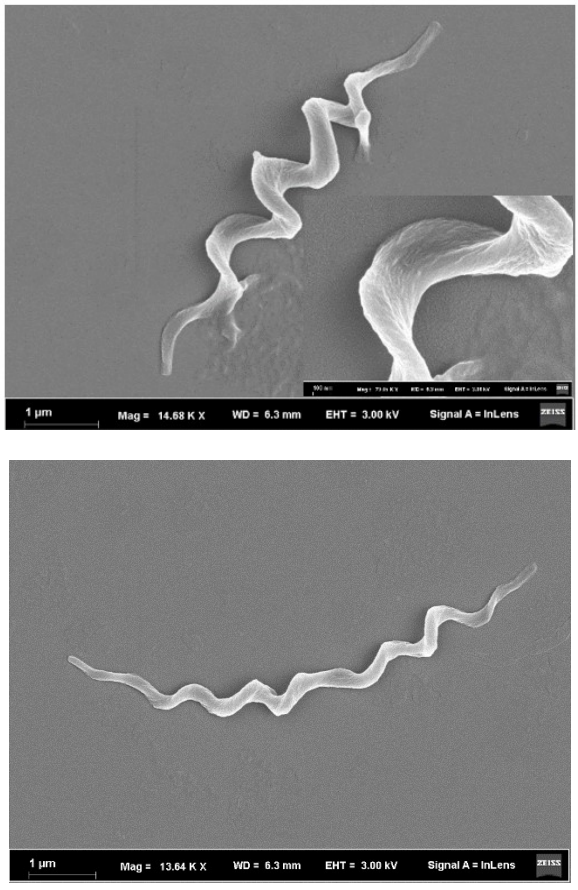

Figure S49. SEM images of **1•2•11** (f_w = 80 vol%, 1:1:1).

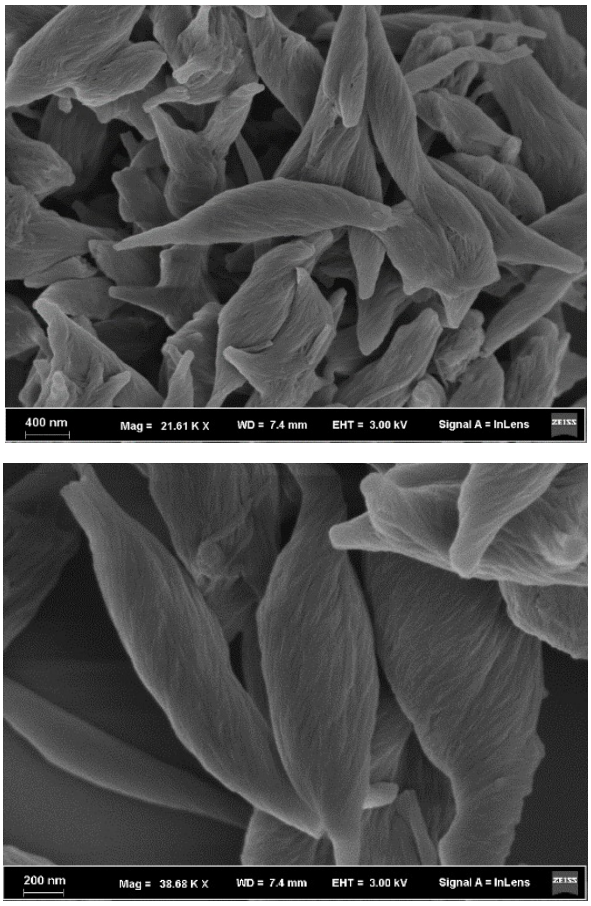

Figure S50. SEM images of **1•12** (f_w = 80 vol%, 1:1).

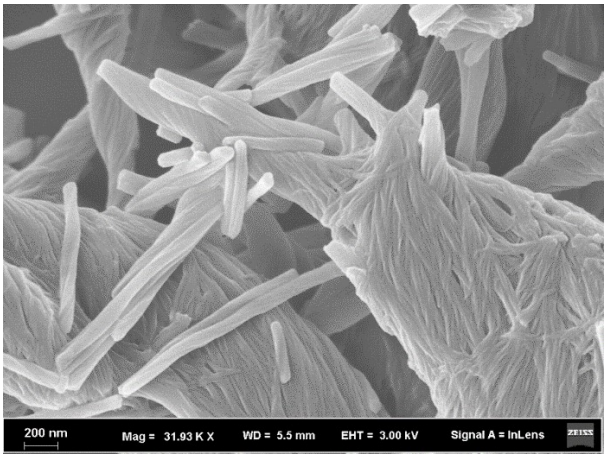

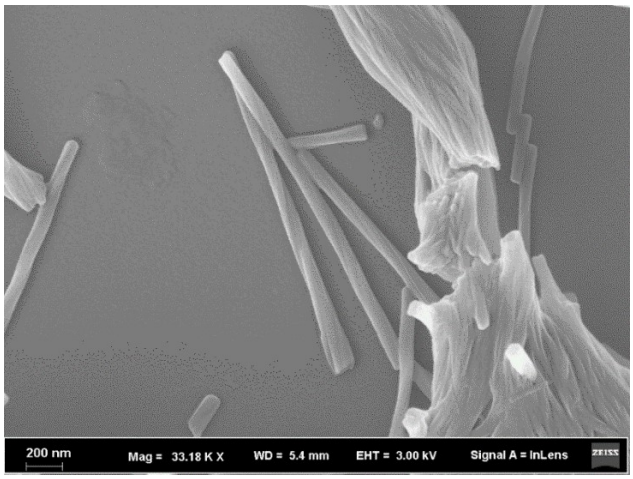

Figure S51. SEM images of **1•2•12** (f_w = 80 vol%, 1:1:1).

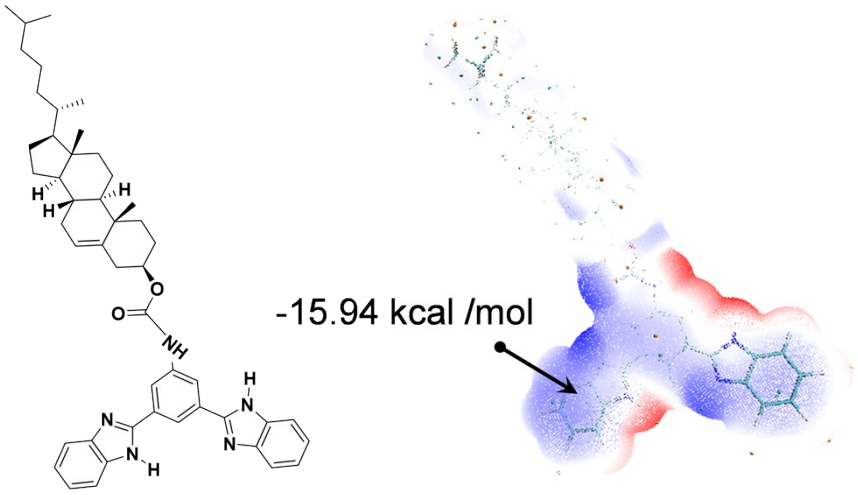

Figure S52. The molecular surface electrostatic potential distribution map of compound **1**.

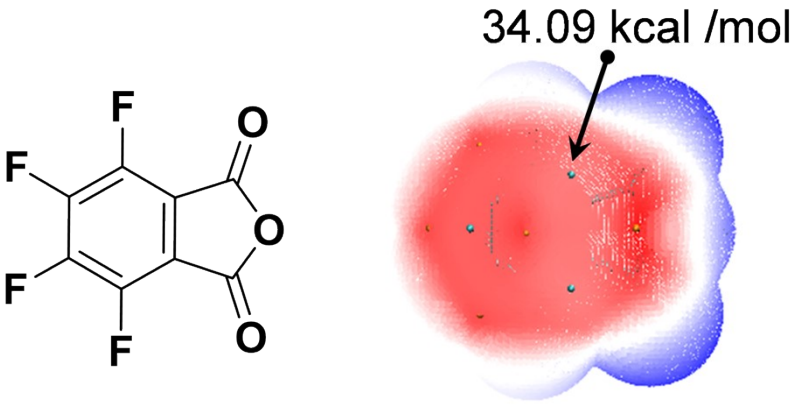

Figure S53. The molecular surface electrostatic potential distribution map of compound **11**.

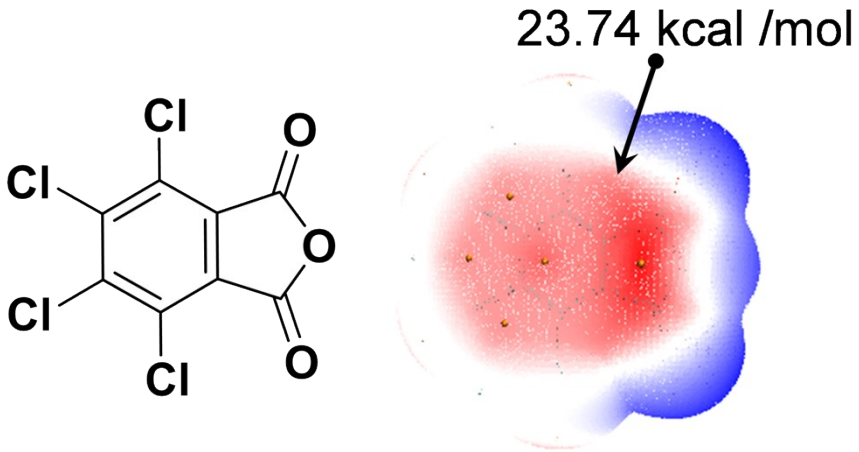

Figure S54. The molecular surface electrostatic potential distribution map of compound **12**.

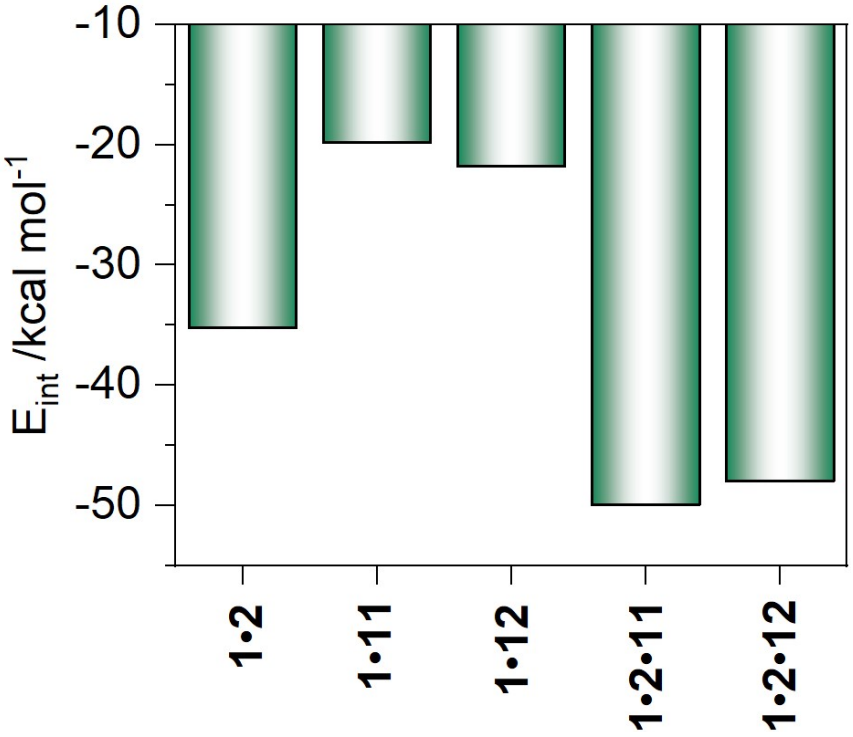

Figure S55: The interaction energies for the formation of the **1•2**, **1•11**, **1•12**, **1•2•11**, and **1•2•12** complexes.